STIFFNESS AND STRENGTH OF STRUCTURAL LAYERS FROM COHESIONLESS MATERIAL

Ulf GERBER[1], Mykola SYSYN[2], Jandab ZAROUR[3], Olga NABOCHENKO[4],

[1, 2, 3] *Technical University of Dresden, Institute of Railway Systems and Public Transport, Dresden, Germany*

[4] *Lviv branch of Dnipropetrovsk National University of Railway Transport, Department of the rolling stock and track, Lviv, Ukraine*

Abstract:

The deformation modulus and permissible stress are two independent parameters that depict the carrying capacity of foundations, including earthworks and ballast layer. Nevertheless, while designing the track superstructure or controlling its state, they are considered separate to each other, even though they are terms of the same measure. The scientific problem is due to the practical necessity of unified building rules and standards. The carrying capacity of earthworks and foundations is regulated with standards based both on deformation and on stress criteria, which are not related to each other. This plays particularly important role for railway ballast layer, as an intermediate between the solids and soil.

The objective of the present research is to estimate the relationship between deformation modulus and the strength of ballast layer. An overview of modern approaches according to the relation between the stiffness, deformation modulus, elasticity and strength of soils and crushed stone is done.

The strength of ballast layer is considered depending on the experimental test: the direct shear test, compressive strength in the uniaxial or biaxial stress state. Load transfer model in crushed stone is proposed. The load transfer angle and cone of loading distribution are determined based on the load transfer and compressive strength models.

The relation between deformation modulus and strength is derived from two simple laboratory experiments with cohesionless ballast material. The experiment tests have shown that the ballast stiffness as well as its strength are influenced with the support stress. The measurement of elastic and residual settlements for the different support stress values enables to determine the relation. It can be potentially used for the development of methods for the ballast compaction control, unification of construction norms. The research result should be considered as an approach for unification of two different ways to reflect the carrying capacity of ballast layer.

Keywords: ballast layer, crushed stone, deformation modulus, strength, carrying capacity

Contact:
1) [https://orcid.org/0000-0002-6101-1390], 2) mykola.sysyn@tu-dresden.de [https://orcid.org/0000-0001-6893-0018] - corresponding author, 3) [https://orcid.org/0000-0003-3558-8660], 4) [https://orcid.org/0000-0001-6048-2556]

1. Introduction

The ballast bed is, simply mechanically considered, cohesionless crushed stone. However, it is the most difficult element of the railway superstructure to understand and predict. Its settlement behavior determines the length of the tamping intervals and thus a significant part of the life cycle costs of the railway superstructure. The settlement behavior results from the relationship between load and load capacity.

Conventionally, the load can be expressed as the mean contact stress between sleeper and ballast, and the load capacity as the corresponding permissible contact stress (Esveld, 2001). This approach derives from the mechanics of materials, which classifies a structure element as stable if the existing stress does not exceed the permissible stress (strength). The similar approach is presented within the phenomenological modelling (Sysyn et al., 2018) of ballast layer settlements with pressure dependent intensity of irreversible deformations.

Soil mechanics deals with the carrying capacity of crushed stone. Here, the ground mechanical state is classified as permissible if the existing stress (load) does not exceed some permissible stress value, that depends on the corresponding deformation modulus (Fendrich and Fengler, 2013). This approach, at first sight, seems strange, because the permissible stress and the elasticity properties of materials are interrelated. Such an approach is not assumed in the mechanics of materials.

The main reason of the discrepancy consists in fact that on the one hand carrying capacity of soils is not constant, but depends on many factors, such as its stress state, compaction (i.e. density), etc. On the other hand, the measurement of soil deformation modulus is the simple practical and reliable non-destructive method to control the quality of earthworks. The different approaches in mechanics of materials and soil mechanics arise from the different structural behavior of solids and crushed stone.

This paper demonstrates the fundamental relationship between deformation modulus and strength as two alternative ways to quantify the carrying capacity of layers from crushed stone using two simple experiments.

The scientific problem is current, and is considered in many recent studies. Authors Rybacki, et al. (2015) have studied the strength and static Young's modulus of shale rocks based experimental triaxial compression tests. The relation of these parameters

to the concept of brittleness is proved and a good, nearly linear, correlation between compressive strength and static Young's modulus was found.

The relationship between the small deformation and strength properties of undisturbed gravelly soils was evaluated within the studies of Enomoto, et al. (2013). The particularity of measurement was the cyclic triaxial compression tests together with dynamic measurements of wave propagation using a pair of accelerometers. The difference between the moduli measured statically and dynamically relating the grain size were discussed. Nabochenko, et al. (2019) and Sysyn, et al. (2019a) study the influence of ballast stiffness on long-term settlements of track and common crossing geometry deterioration with nonlinear dynamic multi-layer beam model. The structural stiffness of track is related to ballast bedding modulus and voids under the sleepers. The influence of crushed stone brakeage on the quality of ballast layer is considered in experimental studies of Fischer, (2017) and Fischer and Juhász, (2019). The ballast settlements in transition areas from ballastless to ballasted track, that are caused with structural stiffness inhomogeneity, are studied by Izvolt, et al., (2016) and Izvolt, et al., (2018). The analysis of ballast behavior under the vibration loading is theoretically studied by Wang, et al., (2016) by means of the discrete element method. The estimation of ballast stiffness change during maintenance works be means of non-destructive seismic methods is proposed in (Sysyn, et al. 2019b).

The relation is used as the basic principle of the strength determination of sedimentary rocks with the measurement of its elastic properties (Umrao, et al., 2018). The data of P-wave velocity together with 45 datasets of other geomechanical properties are used to predict rocks strength with application of artificial neural network and fuzzy logic methods.

The experimental investigation of railway ballast stiffness together with its settlement during 1 million loading cycles was presented by McDowell, et al. (2007). The ballast stiffness, that was measured with non-destructive method – the falling weight deflectometer – has been incremented more than twice after all load cycles. The main problem of the measurement is that it was done for box test without free ballast slopes.

The vertical stiffness of the track, including the stiffness of ballast layer, is considered by many authors (Droździel, et al. 2010, Kovalchuk, et al. 2018,

Grossoni, et al. 2018) as a parameter that characterize the ability of the track to resist to residual deformations.

2. Stability of crushed stone ballast layer
2.1. Direct shear test

Crushed stone, like the ballast bed, has already been destroyed in terms of mechanics of materials. The soil mechanics describes the strength behavior of the crushed rock in a very clear way on the basis of the direct shear test (Fig. 1). The crushed rock located in a horizontally displaceable test facility is subjected to a horizontal force H or shear stress. At the moment when a horizontal movement of the experimental device begins, the shear strength τ_f is reached. However, in contrast to the solid bodies, the strength is not a constant, but changes depending on the vertical force V or the normal stress σ, which acts on the test device. The relationship between strength and normal stress is linear. Two material parameters occur, which are called cohesion c and friction angle φ:

$$\tau_f = c + \sigma \cdot \tan \phi. \tag{1}$$

Cohesion is a measurable value of the adhesive power between the grains. E.g., concrete is a solid that results from the bonding of crushed stone with cement. Thus, its strength is determined mainly by the cohesion. Gravel or sand are typical crushed stones without cohesion. Their strength is simplified described with the relation:

$$\tau_f = \sigma \cdot \tan \phi. \tag{2}$$

Figure 2 illustrates the angle of friction based on Coulomb's friction law (Göbel, 2013), which formulates the permissible shear force T as a function of

the normal force V and the coefficient of friction μ. The resulting force R is inclined by the friction angle φ relative to the vertical force. A coefficient comparison shows that friction coefficient and friction angle are in the relation $\mu = \tan(\Phi)$.
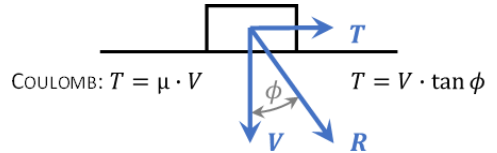

Fig. 2. Friction coefficient μ and friction angle φ

2.2. Compressive strength in the uniaxial stress state

Vertical normal stress σ_z from sleeper on the ballast bed can cause a plastic ballast flow. Ballast flow occurs if the permissible shear stress τ_f is exceeded. This raises the question in which context both variables are related. To find out this, first, the uniaxial stress state is considered, i.e. it is assumed that only a vertical normal stress σ_z acts. The normal and shear stress components (3) of the uniaxial stress state are the function of the intersection angle φ (Fig. 3).

$$\sigma = \sigma_z \cdot \cos^2 \varphi; \quad \tau = \sigma_z \cdot \sin \varphi \cdot \cos \varphi. \tag{3}$$

If one applies τ over σ depending on the intersection angle φ, one obtains the so-called MOHR stress circle (Fig. 4). It is characterized by the fact that the smallest normal stress is zero and the largest normal stress is σ_z.
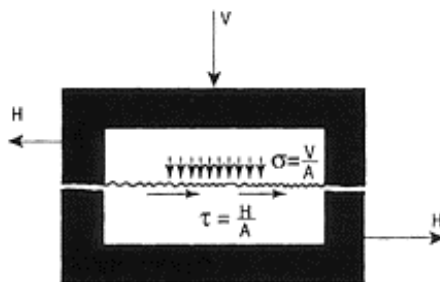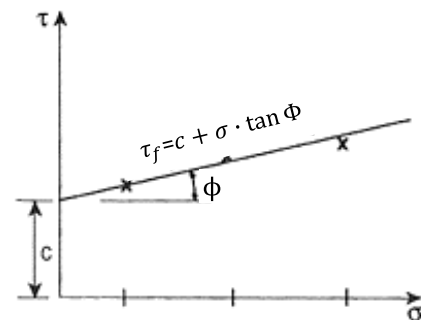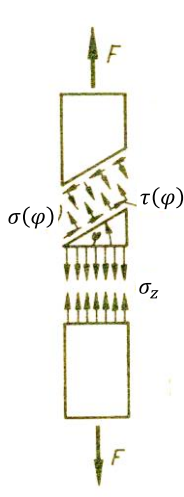

Fig. 1. Direct shear test (Göbel, 2013)

Fig. 3. Stress components in the uniaxial stress state (Göldner 1980)

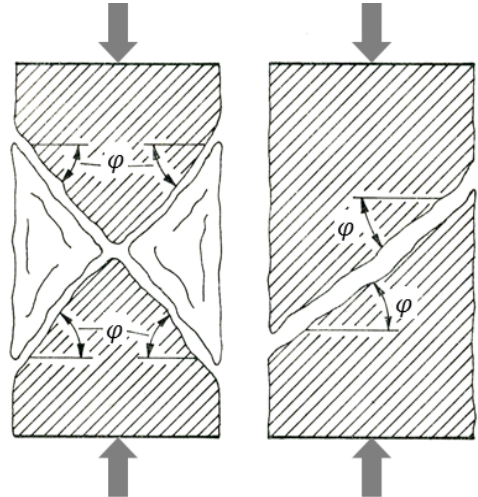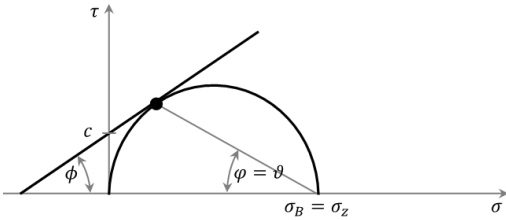Fig. 4. MOHR stress circle and breakline for the uni-axial stress state

A failure occurs when the MOHR stress circle and the break line (strength) determined from the direct shear test come into contact. Since the break line is determined by the material properties (cohesion c and inner friction angle φ), one can choose the diameter of the MOHR circle – i.e. the normal stress σ_z – so that it just almost touches the break line. In the limiting case, the intersection angle assumes the value φ and the normal stress σ_z becomes the maximum compressive stress, i.e. the strength σ_B. This results in the following formula:

$$\sigma_B = \frac{2c \cdot \cos \phi}{1 - \sin \phi}. \qquad (4)$$

The cutting angle can also be experimentally obser-vated on fractured specimens in the case of a uniax-ial stress state (Fig. 5).

Fig. 5. Experimental observation of the cutting angle φ in the uniaxial stress state (Bobe 1983, p. 114)

It is clear from (4) that uniaxial compressive strength exists only in the presence of a cohesion c. However, this does not occur in the ballast bed, so that the rail-way ballast bed has no uniaxial compressive strength.

2.3. Compressive strength in the biaxial stress state

On the basis of the relations of the biaxial stress state (which can be analogously transferred to the actual three-axis stress state), it can be shown that a com-pressive strength of the crushed stone σ_B occurs only in the presence of a horizontal support stress σ_x. For the derivation it is assumed that the vertical normal stress σ_z and the horizontal stress σ_y are the main stress components (Fig. 6).
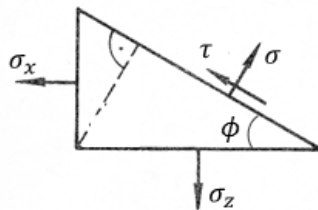

Fig.6. Definition of biaxial stress state (Göldner 1980)

The normal stress component σ and the shear stress component τ of an inclined cutting surface with the intersection angle φ result (Göldner 1980, p. 105):

$$\sigma = \frac{\sigma_x + \sigma_z}{2} + \frac{\sigma_x - \sigma_z}{2} \cos 2\varphi; \quad \tau = -\frac{\sigma_x - \sigma_z}{2} \sin 2\varphi. \quad (5)$$

If one applies τ over σ depending on the cutting angle φ, one obtains the so-called MOHR stress circle for the biaxial stress state (Fig. 7).
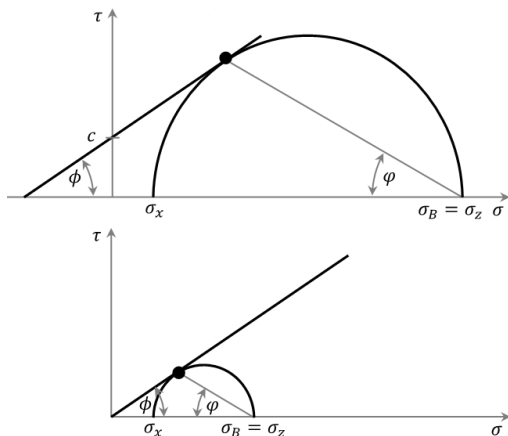

Fig. 7. MOHR stress circle and break line with cohesion (top) and no cohesion (bottom) for the biaxial stress state (Göldner 1980)

In an analogous approach as in the uniaxial stress state, the compressive strength σ_B results in additional dependence on the horizontal support stress σ_x (Fig.7 above). The compressive strength σ_B is identical to the vertical principal stress σ_z:

$$\sigma_B = \frac{2c \cdot \cos \phi}{1 - \sin \phi} + \frac{1 + \sin \phi}{1 - \sin \phi} \cdot \sigma_x. \quad (6)$$

Setting the horizontal support stress to zero results in the uniaxial stress state, that was already derived in (4). In contrast to the uniaxial stress state, materials with no cohesion ($c = 0$) have strength in the biaxial stress state as long as a support stress acts (Fig.7 above):

$$\sigma_B = \frac{1 + \sin \phi}{1 - \sin \phi} \cdot \sigma_x. \quad (7)$$

3. Elasticity of the crushed stone

The linear elasticity of a material, including the crushed stone, is determined by the elastic modulus E [N/mm²]. A horizontal layer of crushed stone is assumed with a height h on a flat, rigid surface; its elastic properties should be calculated, i.e. after its vertical elastic settlement s as a function of the applied vertical stress σ_z, which is lower than the strength σ_B. The relation of both variables gives the bedding modulus C [N/mm³] of ballast bed:

$$C_z = \frac{\sigma_z}{s}. \quad (8)$$

The elastic settlement produces a negative deformation (compression) in the vertical direction:

$$\varepsilon_z = \frac{s}{h}. \quad (9)$$

HOOKE's law combines stress, deformation and modulus of elasticity:

$$\sigma_z = E \cdot \varepsilon_z. \quad (10)$$

By a coefficient comparison of (8) and (10), the modulus of bedding can also be expressed as a function of the elastic modulus:

$$C_z = \frac{E}{h}. \quad (11)$$

Expressing the elastic properties in the form of the vertical elastic settlement as a function of the vertical force F_z, the support point stiffness c_z [N/mm] can be received:

$$c_z = \frac{F_z}{s}. \quad (12)$$

The vertical stress is related to the vertical force on the contact surface A (in railway construction, the sleeper area); in turn, HOOKE's law also applies:

$$\sigma_z = \frac{F_z}{A} = E \cdot \varepsilon_z. \quad (13)$$

Thus, the support stiffness can also be expressed as a function of the modulus of elasticity:

$$c_z = \frac{E \cdot A}{h}. \quad (14)$$

4. Load transfer in crushed stone

The load transfer model answers the question of the spatial distribution of the stress components, which determine the location (sliding line) and the beginning of the flow. The following considerations refer, for simplicity, to the case of a single load acting on an elastic space. Boussinesq (Bobe, 1983) has analytically deduced the stress components for this. According to Fig. 8, the vertical single load V produces in the half-space a vertical normal stress σ_z, the horizontal stresses σ_t and σ_h (which correspond to the horizontal stress σ_x in (7)) and the shear stress τ.
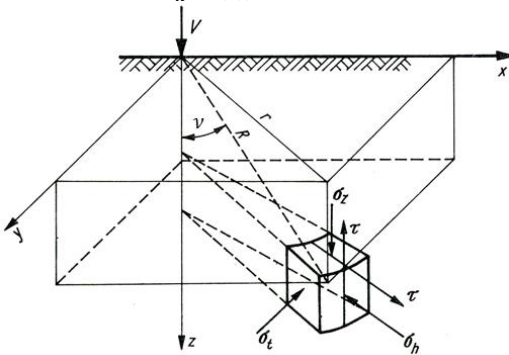

Fig. 8. Definition of the stress components according to Boussinesq (Bobe, 1983)

These stress components are described as a function of their position relative to the individual load V by means of polar coordinates (angle ν and radius R) (Bobe, 1983):

$$\sigma_z = \frac{3 \cdot V}{2\pi \cdot R^2} \cdot \cos^3 \nu \; ; \quad \tau = \frac{3 \cdot V}{2\pi \cdot R^2} \cdot \cos^2 \nu \cdot \sin \nu \; . \quad (15)$$

The ratio of the shear stress τ and the normal stress σ_z follows from this:

$$\frac{\tau}{\sigma_z} = \tan \nu. \quad (16)$$

A coefficient comparison of (16) with the material law from the direct shear test according to (2) shows that the angle ν is identical to the friction angle φ of the crushed stone. It follows that the load transfer occurs within a load transfer cone at the edge of which the yield point of the material is reached (Fig. 9).

The Boussinesq's solution refers to the half-space and explains the load transfer within a load transfer

cone. In the case of railroad ballast, the dimension of the half-plane cannot be considered as infinite. Its free edges are limited with a slope angle (Fig. 10). This raises the question in what relation are the angle of the load transfer cone φ and the ballast slope angle β.
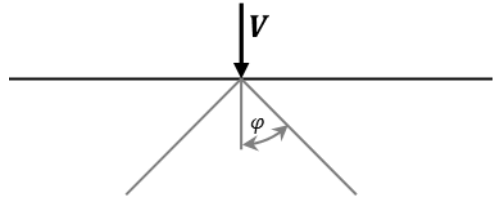

Fig. 9. Load transfer cone according to Boussinesq (Bobe, 1983)
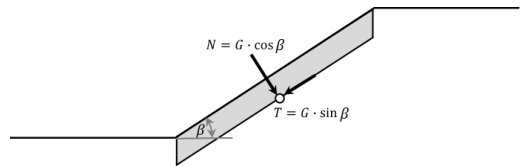

Fig.10. Slope angle

Conferring to Fig. 10, the tangential force component T dependent on the weight G and the normal force component N are inserted into the material law from the direct shear test according to (2). The following equation (17) appears:

$$G \cdot \sin \beta = G \cdot \cos \beta \cdot \tan \phi. \quad (17)$$

According to (17), the shape and load transfer in the railway ballast follows from the identity of the slope angle and the angle of friction $\beta = \varphi$ (Fig. 11).
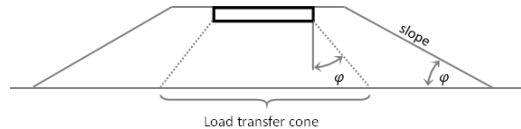

Fig. 11. Load transfer angle and slope angle as a function of the friction angle

5. Experimental determination of deformation modulus and strength

A frame filled with sand under a vertical loading of a square stamp is used as physical model of ballast layer (Fig. 12). The push force F_z and the stamp movement s are measured.
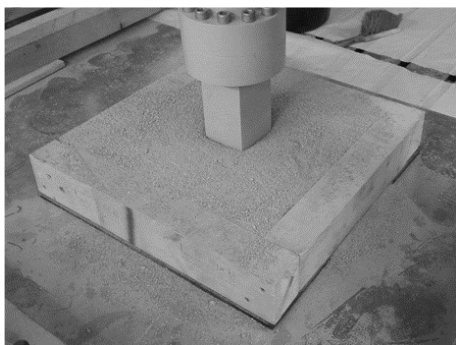
Fig. 12. The experimental setup: part 1

The load consists of cyclical and monotonous increasing parts. Fig. 13 shows the vertical stress σ_z converted to the stamp surface.
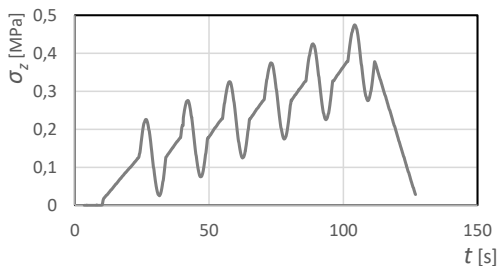

Fig. 13. Vertical stress as a function of time

A second experiment is made with the same loading, which differs from the first one in that the frame has been removed (Fig. 14).
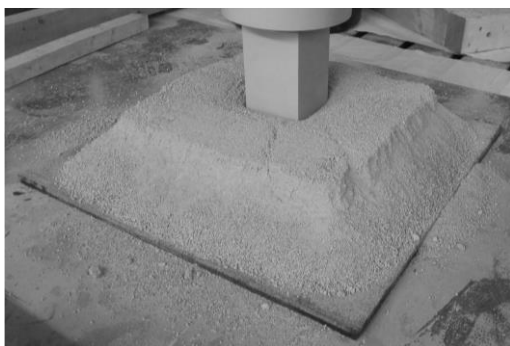

Fig. 14. The experimental setup: part 2

Fig. 15 shows the stamp movement over time. The jump in the stamp settlement indicates that the sand

without frame loses its stability and then assumes a new equilibrium state. In practice this corresponds to a loss of bearing capacity.
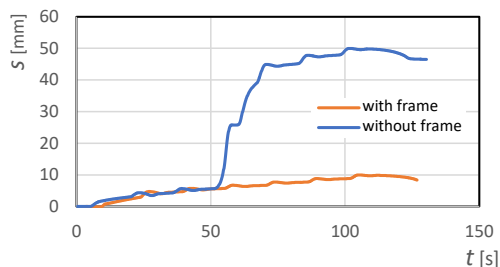

Fig. 15. Stamp settlement as a function of time

Fig. 16 shows the settlement lines of both experiments in comparison. While in the test with frame the strength is greater than the registered maximum stress of 0.48 *N/mm²*, the strength without frame is just under 0.3 *N/mm²*.
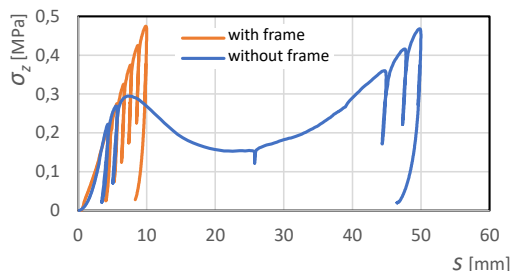

Fig. 16. Stamp pressure depending on the settlement in comparison

To explain the order of magnitude, the average contact stress between threshold and ballast in a conventional railway superstructure should be estimated at this point. An axle load of 200 *kN* generates 2 vertical interpolation forces of 50 *kN*, taking into account the load distribution under the rail. This corresponds to a vertical threshold load of 100 *kN*. In a conventional sleeper geometry (length 2500 *mm*, width 250 *mm*) and the assumption of a uniformly distributed contact stress results a contact stress of $\sigma_z = 0.16$ *N/mm²*. In general, the contact stress distribution between the threshold and gravel is irregular and therefore quickly reaches twice as big value, i.e. the strength limit that has been reached in the experiment without frame. Fig. 17 shows the derivative of

the modulus of deformation $E_{V,i}$ from the working line based on equations (10) and (11) (for each of the $i = 6$ load cycles as shown in Fig. 13, in the experiment: $h = 100\ mm$).
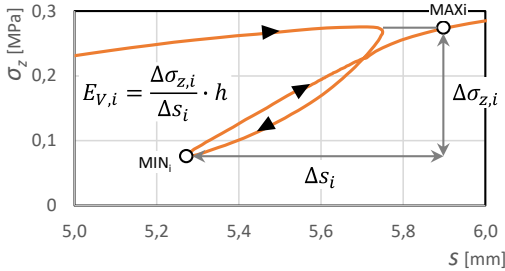

Fig. 17. Derivation of the deformation modulus from the working line

The deformation modulus $E_{V,i}$ can be interpreted as the mean elastic modulus E between the points MINi and MAXi. Fig. 18 shows the comparison of the current deformation modulus $E_{V,i}$ and the current strength $\sigma_{B,i}$. . There is an obvious correlation, which is due to the following linear relationship can be described:
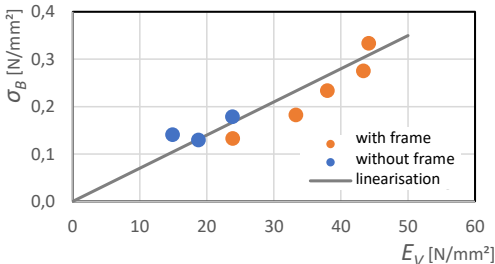
$$\sigma_B = 0,007 \cdot E_V. \tag{18}$$

Fig. 18. Deformation modulus and strength

Each new load cycle according to Fig. 13 results in a compression of the crushed stone. The compression corresponds to the formation of a hydrostatic stress state in the loaded volume below the stamp, i.e. an increase in both the vertical stress σ_z and the support stress σ_x. The support stress could be increased in the experiment without frame only as far as allow the supporting frictional forces of the outer borders. On the other hand, in the test with frame, the support is caused not only the activated frictional

forces of the outer borders, but also the horizontal pressure of the frame. According to equation (7), the strength with frame is larger.

The permissible stress σ_{perm} of consolidated surface protection layers and subgrade is given as a function of the dynamic modulus of elasticity E_{dyn} (Lichtberger 2003, p. 210):

$$\sigma_{perm} = 0,006 \cdot E_{dyn}. \tag{19}$$

The deformation modulus, that is determined according to Figures 17-18 corresponds to a static deformation modulus. The dynamic elastic modulus E_{dyn} is usually around a factor of 1.2 to 2.5 above the static deformation modulus E_V. From a coefficient comparison of (18) and (19), it follows that the safety factor of the condition expressed by equation (19) is 1.4 to 2.9. It should again be noted that the strength according to (18) or the permissible load according to (19), in contrast to solids is not a constant, but depends on the compression, so the size of the existing horizontal support stress. The load capacity, however, depends on the boundary conditions, i.e. from the ability to carry support stresses. This also determines the direction of future work.

6. Conclusions and subsequent studies

The influence of the horizontal support stress on the strength of crushed rock layer is considered. The support stress is built up by the formation of a hydrostatic stress state in the area of the loaded volume. This explains the increase in the deformation modulus with the current vertical stress. This process cased with consolidation. It is finished when slip planes in the crushed rock appear. It is associated with a drastic increase in settlement and is therefore characterized in practice as a loss of carrying capacity.

Between strength and deformation modulus – in contrast to solids – there is a close correlation with crushed rock. As a result of this correlation, it becomes possible to predict the strength of the crushed stones based on their deformation modulus. The advantage of this approach is obvious: the measurements of deformation modulus require minimal effort and are non-destructive. It is shown that the size of the reached compression and thus the size of the reached strength or the reached deformation modulus depends on the horizontal storage conditions of the crushed rock.

The relation found between strength and deformation of ballast layer has a very high practical significance. It can be used for the development of non-destructive methods for the ballast compaction control, unification of construction norms, as well as the strategic maintenance planning and improvement of railway infrastructure (Wieczorek, et al. 2018).

References

[1] BOBE, R., HUBACEK, H., 1983. Soil Mechanics. Berlin: VEB publishing house for construction, 653p.

[2] DROŹDZIEL, J., SOWIŃSKI, B., 2010. Method of track vertical stiffness estimation based on experiment. Archives of Transport, 22(2), pp. 153-162, DOI: 10.2478/v10174-010-0009-y

[3] ENOMOTO, T., QURESHI, O.H., SATO, T., KOSEKI, J., 2013. Strength and deformation characteristics and small strain properties of undisturbed gravelly soils, Soils and Foundations, 53(6), pp. 951-965, DOI: 10.1016/j.sandf.2013.10.004

[4] ESVELD, C., 2001. Modern Railway Track. Second Edition, MRT-Production, Zaltbommel, The Netherlands, 653 p.

[5] FENDRICH, L., FENGLER, W., 2013. Handbuch Eisenbahninfrastruktur (Handbook Railway Infrastructure), Springer-Verlag Berlin Heidelberg, 1105 p. doi.org/10.1007/978-3-642-30021-9

[6] FISCHER, S., 2017. Breakage Test of Railway Ballast Materials with New Laboratory Method. Periodica Polytechnica Civil Engineering, 61(4), 794-802. DOI: 10.3311/PPci.8549.

[7] FISCHER, S., JUHÁSZ, E., 2019. Railroad Ballast Particle Breakage with Unique Laboratory Test Method, Acta Technica Jaurinensis, 12(1), 26-54. DOI: 10.14513/actatechjaur.v12.n1.489.

[8] GÖBEL, C., FISCHER, R., LIEBERENZ, K., 2013. Handbuch Erdbauwerke der Bahnen Planung, Bemessung, Ausführung,Instandhaltung. Eurailpress, 2013, 551 p. ISBN-10: 3777104302

[9] GÖLDNER, H., HOLZWEIßIG, F., 1980. Guidelines for Technical Mechanics. Leipzig: VEB book publisher Leipzig, 667 p.

[10] GROSSONI, I., ANDRADE, A., BEZIN, Y., NEVES, S., 2018. The role of track stiffness and its spatial variability on long-term track quality deterioration. Proc IMechE Part F: J Rail and Rapid Transit 233(1) pp. 16–32. DOI:10.1177/0954409718777372.

[11] IZVOLT, L., HARUSINEC, J., SMALO, M., 2018. Optimisation of transition areas between ballastless track and ballasted track in the area of the tunnel Turecky vrch. COMMUNICATIONS Scientific Letters of the University of Zilina, 20(3), 67-76.

[12] IZVOLT, L., SESTAKOVA, J., SMALO, M., 2016. Analysis of results of monitoring and prediction of quality development of ballasted and ballastless track superstructure and its transition areas. COMMUNICATIONS Scientific Letters of the University of Zilina. 18(4):19-29.

[13] KOVALCHUK, V., KOVALCHUK, Y., SYSYN, M., STANKEVYCH, V. AND PETRENKO, O., 2018. Estimation of carrying capacity of metallic corrugated structures of the type multiplate mp 150 during interaction with backfill soil. Eastern-European Journal of Enterprise Technologies. Kharkov: 1/1 (91), pp. 18-26, doi: 10.15587/1729-4061.2018.123002.

[14] LICHTBERGER, B., 2003. Handbuch Gleis: Unterbau, Oberbau, Instandhaltung, Wirtschaftlichkeit (Track Compendium: Formation, Permanent Way, Maintenance, Economics). Hamburg: Tetzlaff Verlag, 656 p.

[15] MCDOWELL, G.R., LIM, W.L., COLLOP, A.C., ARMITAGE, R., THOM, N.H., 2007, Laboratory simulation of train loading and tamping on ballast. Proceedings of the Institution of Civil Engineers: Transport, 158(2), pp. 89-95, DOI: 10.1680/tran.2005.158.2.89

[16] NABOCHENKO, O., SYSYN, M., KOVALCHUK, V., KOVALCHUK, YU., PENTSAK, A., BRAICHENKO, S., 2019. Studying the railroad track geometry deterioration as a result of an uneven subsidence of the ballast layer, Eastern-European Journal of Enterprise Technologies, 1/7 (97), 50-59. DOI: 10.15587/1729-4061.2019.154864

[17] RYBACKI, E., REINICKE, A., MEIER, T., MAKASI, M., DRESEN, G., 2015. What controls the mechanical properties of shale rocks? – Part I: Strength and Young's modulus, Journal of Petroleum Science and Engineering, 135, pp. 702-722, 2015, DOI: 10.1016/j.petrol.2015.10.028

[18] SYSYN, M., GERBER, U., GRUEN, D., NA-BOCHENKO, O., KOVALCHUK, V., 2019a. Modelling and vehicle based measurements of ballast settlements under the common crossing. European Transport, 71(5), 1-25.

[19] SYSYN, M., GERBER, U., KOVALCHUK, V., NABOCHENKO, O., 2018. The complex phenomenological model for prediction of inhomogeneous deformations of railway ballast layer after tamping works. Archives of Transport, 47(3), pp. 91-107. DOI: https://doi.org/10.5604/01.3001.0012.6512

[20] SYSYN, M., NABOCHENKO, O., GERBER, U., KOVALCHUK, V. 2019b. Evaluation of railway ballast layer consolidation after maintenance works. Acta Polytechnica, 58(6), 77–87. DOI: 10.14311/AP.2019.59.0077

[21] UMRAO, R.K., SHARMA, L.K., SINGH, R., SINGH, T.N. 2018. Determination of strength and modulus of elasticity of heterogenous sedimentary rocks: An ANFIS predictive technique, Measurement: Journal of the International Measurement Confederation, 126, pp. 194-201, DOI: 10.1016/j.measurement.2018.05.064

[22] WANG, B., MARTIN, U., RAPP, S. 2016. Vibration characteristic analysis of ballast with different aspect ratios by means of the discrete element method. Geotechnical Special Publication, (268 GSP), 16-23.

[23] WIECZOREK, S., PAŁKA, K., GRABOWSKA-BUJNA, B. 2018. A model of strategic safety management in railway transport based on Jastrzebska Railway Company Ltd. Scientific Journal of Silesian University of Technology. Series Transport. 2018, 98, pp. 201-210. ISSN: 0209-3324. DOI: 10.20858/sjsutst.2018.98.19.